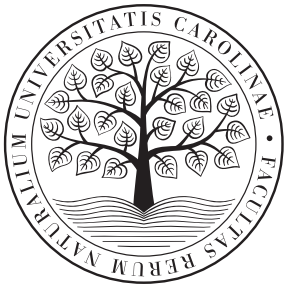

FACULTY OF SCIENCE
Charles University

BACHELOR THESIS

Marek Tobiáš

Biophysical Conditions Triggering Depolarization Block in Excitatory Neurons

Biofyzikální podmínky spouštějící depolarizační blok v excitačních neuronech

Department of Cell Biology

Supervisor of the bachelor thesis: David Maximilian Berling, M.Sc.

Study programme: Bioinformatics

Study branch: B-BINF

Prague 2024

Prohlašuji, že jsem tuto bakalářskou práci vypracoval samostatně a výhradně s použitím citovaných pramenů, literatury a dalších odborných zdrojů. Velké jazykové modely byly využity především ke zlepšení srozumitelnosti určitých vět. Tato práce nebyla využita k získání jiného nebo stejného titulu.

Beru na vědomí, že se na moji práci vztahují práva a povinnosti vyplývající ze zákona č. 121/2000 Sb., autorského zákona v platném znění, zejména skutečnost, že Univerzita Karlova má právo na uzavření licenční smlouvy o užití této práce jako školního díla podle §60 odst. 1 autorského zákona.

V ..... dne ....

Podpis autora

I dedicate this thesis to my family and friends for their constant support and encouragement.

I would also like to express my gratitude to my supervisor, David Maximilian Berling, M.Sc., for his guidance and invaluable advice on academic writing throughout this project.

Title: Biophysical Conditions Triggering Depolarization Block in Excitatory Neurons

Abstract: Optogenetics is an increasingly popular neuronal stimulation technique used for studying neural circuits and controlling brain activity. However, when applied without sufficient knowledge, it can cause unintentional silencing of the targeted neurons by inducing a state termed depolarization block (DpB), in which neurons cease to fire action potentials. The susceptibility to silencing is not consistent among neurons, and the relationship between their biophysical properties and their vulnerability to DpB remains poorly understood. In this thesis, we investigate how the densities of voltage-gated sodium (Na_v) and potassium (K_v) channels, which are known to govern DpB dynamics, influence the neuron's ability to resist this phenomenon. We also examine the impact of neuronal size on DpB susceptibility. Using a computational model of a layer V pyramidal neuron, which we simplify to a single compartment to represent the behavior of a generic excitatory neuron, we introduce an automatic classifier consistently identifying DpB through voltage trace analysis. This allows us to systematically assess the influence of varying Na_v or K_v channel densities in the neuron's membrane. We discover that increasing these densities enhances the neuron's resistance to DpB. Contrary to previous studies, neuronal size was found not to affect susceptibility to light-induced DpB. Furthermore, our analysis shows that while increasing Na_v channel density raises the mean of depolarized membrane voltage at which DpB settles, K_v channel density affects this property only if the membrane contains intermediate densities of Na_v channels.

Keywords: Depolarization block, Simulation, Neuron model, Optogenetic stimulation

Název: Biofyzikální podmínky spouštějící depolarizační blok v excitačních neuronech

Abstrakt: Optogenetika je stále oblíbenější technikou stimulace neuronů používanou ke studiu nervových obvodů a k řízení mozkové aktivity. Nicméně, pokud je aplikována bez dostatečných znalostí, může neúmyslně umlčet aktivitu stimulovaných neuronů tím, že v nich spustí depolarizační blok (DpB) - stav, při kterém neurony ztrácí schopnost vést vzruchy, a proto i komunikovat. Mezi neurony se náchylnost k umlčení liší, a navíc je stále málo zmapované, jak jejich biofyzikální vlastnosti ovlivňují citlivost ke spuštění DpB. V této práci zkoumáme, jak hustota napěťově řízených sodíkových (Na_v) a draselných (K_v) kanálů, stojících za mechanismem způsobujícím DpB, ovlivňuje schopnost neuronu tomuto jevu odolávat. Dále zkoumáme i vliv velikosti neuronu. Pomocí simulace výpočetního modelu pyramidového neuronu páté vrstvy, který jsme zredukovali pouze na tělo neuronu, reprezentujeme chování obecného excitačního neuronu. Vytvoříme automatický klasifikátor, identifikující DpB ze simulovaných napěťových stop, který nám umožní systematicky vyhodnotit vliv specifických kombinací hustot Na_v a K_v kanálů v membráně neuronu. Zjistili jsme, že zvýšení těchto hustot zvyšuje odolnost neuronu vůči DpB. Na rozdíl od předchozích studií zjišťujeme, že náchylnost k světlem indukovanému DpB není ovlivněna velikostí neuronu. Naše analýza dále ukazuje, že zatímco zvyšování hustoty Na_v kanálů zvedá hodnotu průměrného napětí, na které se blok ustálí, hustota K_v kanálů ji ovlivňuje pouze, pokud má membrána střední úrovně hustoty Na_v kanálů.

Klíčová slova: depolarizační blok, simulace, neuronový model, optogenetická stimulace

Contents

1. Introduction

Neurons, often labeled as the fundamental building blocks of the nervous system, play an essential role in transmitting signals across the brain. These seemingly simple processing units form networks that give rise to complex behaviors such as learning, perception and thought formation. Understanding how neurons represent and process information - neural coding - is essential for further advances in both research and medical practice. To study these cells, researchers have come up with diverse approaches. One involves observing and measuring their membranes' electrophysiological properties, namely the voltage.

The typical behavior of a neuron is seen as integrating incoming signals and, if stimulated enough, firing an action potential (AP) as an outgoing signal, which is a spike in the membrane's voltage. This signal leaves the neuron through a protrusion of the neuron's body, called the axon, which connects the neurons to one another, forming a network. (Bear et al., 2016)

Stimulating neurons is key to controlling neural activity, enabling researchers to access the underlying processes of perception, cognition, and behavior. By targeted activation or inhibition of specific neurons, scientists can discover the roles these cells play. This capability is crucial for understanding how brain regions interact, how neural circuits contribute to psychological and physiological functions, and how disruptions in these processes drive neurological disorders. Moreover, neuronal stimulation is essential for advancing therapeutic strategies, such as deep brain stimulation for managing Parkinson's disease (Benabid, 2003) or neuroprosthetic devices, providing the ability to repair or replace lost sensory and motor functions (Barrett et al., 2014; Kleinlogel et al., 2020; Sahel et al., 2021).

To see how a single neuron reacts to specific intensities of different inputs, scientists have used direct current to mimic incoming signals. In addition to stimulation with direct current, the discovery of the **optogenetic approach** - a new external stimulation method which uses light as a stimulant - has enriched the scientific toolbox, rendering direct current as less specific and less precise (Boyden et al., 2005). Optogenetic stimulation activates genetically modified cells that express light-sensitive proteins that open when exposed to light. This enables precise genetic targeting - optogenetic stimulation is, therefore, advantageous in its specificity and has high temporal and spatial precision (Boyden et al., 2005; Deisseroth, 2015). This advancement led to a more rigorous understanding of neural circuits in general (Deisseroth, 2015; Emiliani et al., 2022). However, to precisely stimulate many neurons at once in patterns that drive specific circuit behavior, researchers need to know how every single one reacts.

Upon investigating the effects of extreme stimulation conditions, researchers have observed that the neuron's ability to fire APs gets blocked, a phenomenon termed **depolarization block** (DpB). Often considered a pathological condition, its properties and function are not sufficiently understood. It has already been described that the event depends on an individual neuron's type, morphology, and inner properties, making it difficult to study due to the dimensionality of the mentioned contributing factors (Mattis et al., 2012; Herman et al., 2014).

To better understand what is happening in the neuron during the stimulation itself, *in silico* models have been created, forming a basis of a qualitative, non-invasive approach. These models are especially beneficial in comparison to *in vivo* experiments, which frequently pose a time-consuming challenge for researchers and do not permit the real-time observation and modification of various neuronal properties.

1.1 Outline and Goals

In this thesis, we simulate optogenetic stimulation of a simplified neuronal model to map and understand the biophysical conditions at which DpB occurs. A superior comprehension of this phenomenon can lead to an improved insight into various neurological states as well as more informed stimulation parameters in researchers' experiments, thus refining the quality of the results.

We establish a robust biological background, describing the characteristics of excitatory neurons. We summarize mechanisms behind the generation of APs, emphasizing the critical roles played by voltage-gated sodium (Na_v) and potassium channels (K_v).

We introduce the reader to the mathematical description of AP initiation and propagation through the Hodgkin-Huxley model (Hodgkin and Huxley, 1952). We investigate the principles of optogenetics, analyze the mechanisms underlying the DpB condition (Bianchi et al., 2012), and review the differences in susceptibilities to this state, highlighting the diverse electrophysiological responses among neuronal subtypes (Herman et al., 2014).

We utilize and reduce a model of layer V (L5) pyramidal neuron, which already incorporates an existing light-source framework (Berling et al., 2024).

Acknowledging that Na_v and K_v channels are sufficient to explain DpB dynamics (Bianchi et al., 2012), we pursue the following goals:

- **G_0:** To compare DpB across neuron's biophysical conditions computationally, we need a formal DpB definition and an automatic classifier of DpB based on simulated voltage traces.
- **G_1:** We aim to determine whether and how the densities of Na_v or K_v channels in the neuron's membrane affect the onset of DpB. Understanding this could help us predict responses of neuronal subtypes with known densities.
- **G_2:** Motivated by the assumption that interneurons are more susceptible to DpB than excitatory neurons because of their smaller size, we investigate whether the size of the neuron subjected to optogenetic stimulation plays a role.
- **G_3:** We explore the depolarized membrane voltage level at which a neuron in a DpB condition stabilizes since when evaluating DpB voltage traces, we found that the amount of depolarization characteristically differs between roughly two states. We want to understand whether and how Na_v and K_v channel densities relate to this.

Our findings reveal that higher densities of Na_v or K_v channels require increased stimulation intensity to induce DpB. We also discover that the size of the neuron has minimal impact on this phenomenon under light stimulation, and the value of the membrane voltage at which the neuron in DpB stabilizes depends solely on the density of Na_v channels, except a region of intermediate Na_v densities where K_v channels influence the equilibrium value.

2. Background

2.1 Neuron

A neuron is a highly specialized cell designed to transmit information through electrical and chemical signals. At the heart of neuronal functionality is the concept of membrane voltage, also known as the membrane potential - an electrical potential difference across the neuron's membrane. Membrane voltage is not static - it varies in response to the neuron's activity and the surrounding ionic environment, working as a dynamic indicator of the neuron's state. (Alberts, 2022)

The significance of membrane voltage in excitable cells lies in its role in generating action potentials (APs), which are rapid changes in voltage that propagate along the neuron's axon to communicate with other neurons, muscles, or glands. These voltage changes are organized by the movement of ions through static and dynamically opening ion channels, pumps, or leaks in the neuronal membrane. (Hodgkin and Huxley, 1952; Bear et al., 2016)

2.1.1 Ion channels and pumps

Specifically, sodium (Na^+), potassium (K^+) channels and the Na^+/K^+ pump are crucial for the generation and propagation of APs in neurons. These protein structures embedded in the cell's membrane serve as conduits for ion passage regulation. (Hodgkin and Huxley, 1952; Alberts, 2022)

Voltage-gated sodium channel

Sodium channels are integral membrane proteins that facilitate the influx of Na^+ ions, triggering depolarization - an increase in membrane voltage. Fundamental drivers of rapid depolarization in the generation of an AP are the voltage-gated sodium channels (Na_v). In general, Na_v channels are transient - they open briefly in response to stimulus and are sometimes referred to as NaT channels. (Bear et al., 2016)

Structurally, Na_v channels are composed of a large alpha subunit that forms the pore, through which ions pass, and beta subunits that modulate the channel's biophysical properties. The alpha subunit, which forms the pore, is characterized by its four distinct domains (I-IV), each containing six transmembrane segments (S1-S6). The S4 segments act as a voltage sensor, possessing positively charged residues that respond to changes in membrane potential. Upon depolarization, the movement of the S4 segments triggers the opening of the channel's pore. This pore is highly selective for Na^+ ions - specificity made possible by the selectivity filter formed by the loop between S5 and S6, located at the pore's outer mouth. (reviewed by Yu and Catterall, 2003; Bear et al., 2016)

Na_v channel gating — transitioning between **open**, **closed**, and **inactivated states** — is modulated by the channel's voltage-sensor, which consequently allows Na^+ influx, followed by a fast inactivation of the channel (Hodgkin and Huxley, 1952; reviewed by Yu and Catterall, 2003; Bear et al., 2016). The inactivation alters the channel's conformation, plugging the channel's intracellular

mouth ('ball and chain' mechanism). This is likely mediated by a particular motif in the linker connecting domains III and IV (Goldin, 2003). The channel is de-inactivated - driven from inactivated to closed state - when around or below its resting potential.

Voltage-gated potassium channel

Potassium channels are, among other things, critical for decreasing the membrane voltage (hyperpolarizing) after rapid depolarization and maintaining the neuron's resting potential, around -65 mV (Bear et al., 2016). Gated potassium channels can be broadly categorized into two categories based on their topology - voltage-gated potassium channels (K_v) and inward-rectifier potassium channels (K_{ir}) (Miller, 2000). In the context of generating an AP, K_v channels play an essential role, providing a rapid outward flow of K^+ ions (Bear et al., 2016). These K_v channels, unlike Na_v channels' transient property, open with a delay and are, therefore, sometimes called delayed-rectifier K_v channels (K_{DR}) (Bear et al., 2016).

K_v channels consist of four subunits that come together to form a pore. Each subunit has six transmembrane segments (S1-S6), with the S4 segments serving as the voltage sensor. These channels open in response to membrane depolarization but with slower kinetics than Na_v channels. The selectivity filter, located at the narrowest part of the pore, precisely distinguishes K^+ ions from other ions based on size and hydration energy, allowing rapid K^+ throughput. (Miller, 2000; Kim and Nimigean, 2016)

Unlike Na_v channel, K_v channel gating can be understood as transitioning between two states only - **open** and **closed** (Hodgkin and Huxley, 1952), which are regulated by the channel's voltage sensor as well. These channels do not close after single ion passage but rather remain open until membrane potential decreases.

Na^+/K^+ pump

Also known as the sodium-potassium ATPase, it is a membrane protein that plays a crucial role in maintaining the cell's resting potential and ionic balance. This pump operates through an active transport mechanism, using ATP (adenosine triphosphate) to move ions against their concentration gradients. For every cycle, it transports three Na^+ ions out of the cell and two K^+ ions into the cell. This activity establishes a high concentration of Na^+ ions outside the cell and a high concentration of K^+ ions inside the cell, resulting in negative resting membrane potential that is essential for the function of neurons - maintaining electrochemical gradients necessary for the generation of APs and for the conservation of cell's homeostasis. (Bear et al., 2016)

2.1.2 Dynamics

The membrane potential dynamics can be reduced to the phases explained below (illustrated in Fig. 2.1).

- **Resting State**: The neuron's resting membrane potential, of approximately -65 mV, is primarily maintained by the balance between the uneven

distribution of ions across the membrane and the activity of the Na^+/K^+ pump. This equilibrium arises as concentration and electrical gradients counterbalance each other. (Bear et al., 2016; Alberts, 2022)

- **Depolarization period**: The AP begins when the neuron receives a stimulus strong enough to cause a significant depolarization, typically reaching the threshold of -55 to -50 mV (Seifter et al., 2005). This depolarization opens Na_v channels, allowing Na^+ ions to rush into the cell, causing the membrane potential to become rapidly more positive (Bear et al., 2016).

- **Peak Phase**: As the membrane potential approaches +40 mV, Na_v channels are mostly all inactivated, and K_v channels open. This results in the efflux of K^+ ions, initiating the process of repolarizing the membrane back toward its resting potential.

- **Repolarization**: The outflow of ions through K_v channels continues until the membrane potential returns to a more negative value, slightly overshooting below the resting potential value due to the delayed closing of K_v channels (Bear et al., 2016). This period is known as the hyperpolarization period.

- **Refractory Period**: During this phase, the neuron is less susceptible to new stimuli, ensuring that the AP moves in one direction along the neuron. The Na^+/K^+ pump restores the original ion distribution, returning the neuron to its resting state and preparing it for another AP. We recognize two types of refractory periods - *absolute* and *relative*. The absolute refractory period takes place immediately after the firing of an AP and is characterized by the complete inability to generate another AP, no matter how strong the stimulus is. During the relative refractory period, on the other hand, the neuron can fire another AP, however, it is harder than normally, as a portion of K_v channels remains open and Na_v channels are still recovering from inactivated to the closed state. Further, the membrane potential is experiencing an undershoot. This together means that any incoming stimulus will be counteracted by K^+ efflux, diminished by an insufficient number of Na_v channels available or simply has to travel a greater distance to the threshold voltage due to undershooting. Bear et al., 2016

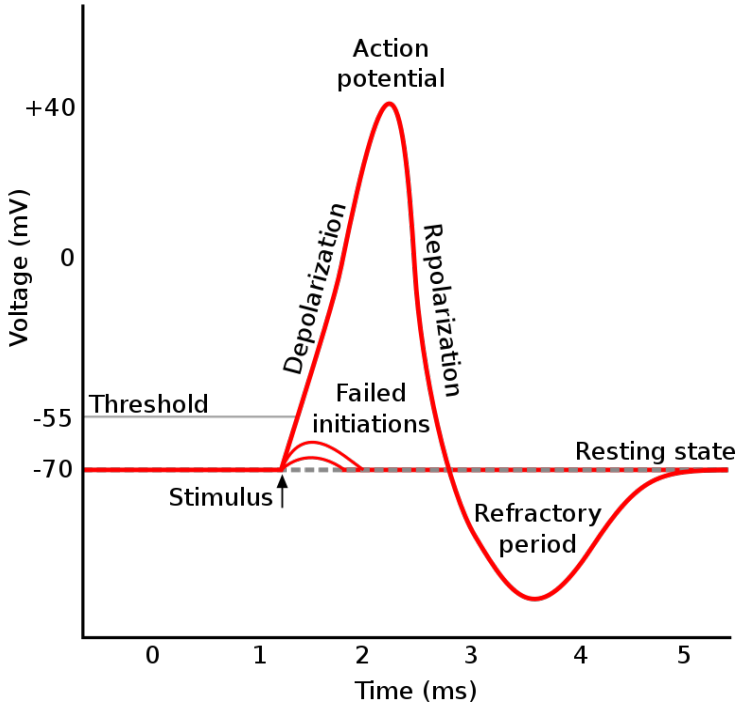

Figure 2.1: **Membrane voltage trace during action potential generation.** Input from other neurons can elevate the membrane voltage past the threshold, triggering an AP. The initiation fails with insufficient input. Following the AP, the voltage undershoots below the resting potential during a phase known as the refractory period. Initially, during this period, it is impossible to generate another AP and subsequently, generating an AP requires more input than in the resting state. The membrane voltage slowly resets to the resting potential value. Taken from Wikimedia Commons, distributed under CC-BY 2.0 license.

2.1.3 Processing

A neuron's ability to process information is modulated by the strength and timing of inputs, the integration of excitatory and inhibitory signals, and the neuron's intrinsic properties, such as ion channel distribution and membrane potential.

At the beginning of each communication process are the presynaptic neurons, which release neurotransmitters into the synaptic cleft, and the postsynaptic neurons, which receive these chemical signals through receptor activation. This interaction determines whether the postsynaptic neuron will be pushed closer to or further from threshold potential, thus regulating its excitability. Signals received by the postsynaptic neuron can be excitatory, which increase the neuron's activity, or inhibitory, which reduce it. The dynamic balance between these two types of inputs shapes the output of neural networks, enabling complex behaviors, learning, and memory formation. (Bear et al., 2016)

2.1.4 Excitatory neuron

An excitatory neuron is a type of neuron that, upon activation, increases the likelihood of postsynaptically connected neurons to fire an AP. They typically

release excitatory neurotransmitters such as glutamate, which binds to receptors on the postsynaptic neuron, causing depolarization and promoting AP initiation. (Alberts, 2022)

A particularly abundant excitatory neuron within the cortex is the layer V (L5) pyramidal neuron. L5 pyramidal neurons are distinguished by their large size, extensive dendritic tree, and long axons that can extend to different cortical and subcortical areas, making them integral in cortical processing and output (see Fig. 2.2). They are involved in various functions, including motor control and sensory processing. (Bear et al., 2016)

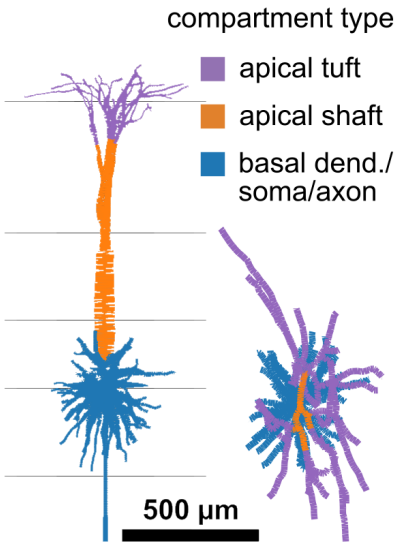

Figure 2.2: **Schematic of a layer V pyramidal neuron.** Apical tuft (purple), apical shaft (orange), and the rest of neuron's morphology (blue) of the L5 pyramidal neuron inside the cortex viewed from the side with horizontal lines representing cortical layers **(left)** and the same neuron viewed from the top of the cortex **(right)**. Figure adapted from Berling et al., 2024.

2.2 Hodgkin-Huxley model

Based on experiments with the giant axon of the squid, this model describes how APs in neurons are generated and propagated. It mathematically represents the voltage or ion dynamics along the neuron's membrane, describing the inner workings of specific ion channels, namely Na_v, K_v, and a leak channel, which is representative of all other channel types not described explicitly, linking ion channel dynamics with the electrical behavior of neurons by modeling the neuron's membrane as an electrical circuit (Fig. 2.3). (Hodgkin and Huxley, 1952)

The cell's membrane is represented by a capacitor (C), which stores electric energy and separates electric charges. Ion channel dynamics are reduced to resistors (R) connected in parallel, with the leak channel being the only one with constant resistance, thus symbolizing an invariant open state where ions move through with conductance $g = \frac{1}{R}$. Each channel is further described by a battery voltage (E), denoting channel-specific Nernst potentials, where the Nernst potential for each type of ion is the membrane potential at which there is no net

flow of that ion in or out of the cell (Bear et al., 2016). Our variable of interest is the voltage across the membrane, denoted as u.

The membrane is injected with current I, causing a temporal change in the electric field - i.e., symbolizing incoming signals from other neurons. The injected current is then distributed across the capacitor and all the channels. This can be denoted mathematically as $I(t) = I_C(t) + \sum_k I_k(t)$, with k representing $\mathrm{Na_v}$, ($\mathrm{K_v}$), and leak conductance. To calculate the change in membrane potential, we rewrite the equation as

$$C\frac{du}{dt} = I(t) - \sum_k I_k(t).$$

The sum of channel currents can be expanded in the following way

$$\sum_k I_k(t) = g_{Na}m^3h(u - E_{Na}) + g_K n^4(u - E_K) + g_L(u - E_L),$$

where g_X and E_X are channel specific conductances and battery voltages respectively. The initial success of this model lay in variables m, n, h - **gating variables**, which model the probability that a channel is open at a given moment in time, where n is the probability of a $\mathrm{K_v}$ channel in an open state, and m and h combined define the gating of $\mathrm{Na_v}$ channel, m being the activation and h the inactivation variable. These are understood as evolving around following differential equations, where x is an opening variable and $x_0(u)$ a target value which x approaches with a time constant $\tau_x(u)$ (Gerstner, 2014)

$$\frac{dx}{dt} = -\frac{1}{\tau_x(u)}(x - x_0(u)).$$

These equations collectively describe what is referred to as the standard Hodgkin-Huxley model. This model can be further expanded - more complex frameworks already exist (Forrest, 2014; Nandi et al., 2022). It is important to note that the voltage trace's smoothness achieved with this model is not realistic - transitioning between open and closed states of individual channels is stochastic - m, n, h can be viewed as variables acquired from averaging over many experiments. *In vivo* experimental data can exhibit greater variability and irregularity (Bear et al., 2016).

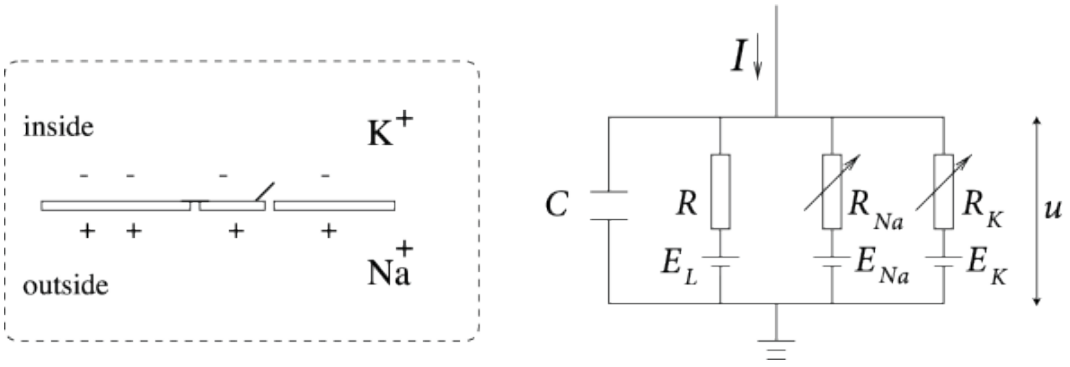

Figure 2.3: **Schematic of ion distributions across a neuron's membrane and Hodgkin-Huxley's representation as an electrical circuit.** A diagram depicting the cell's interior and exterior, highlighting the membrane's charge on both sides, where K^+ concentration is shown as being higher inside the cell, while Na^+ is more concentrated outside **(left)**. A circuit illustrating the distribution of current upon injection into the membrane, where C represents the membrane as a capacitor, and channel-specific resistors R and batteries E collectively describe specific channel dynamics, and u represents the voltage across the membrane **(right)**. Taken from Gerstner, 2014.

The Na^+/K^+ pump is not explicitly modeled as it mainly evens out chemical concentrations that are not specifically tracked (Hodgkin and Huxley, 1952).

2.3 Optogenetic stimulation

Optogenetics is a biological technique that uses light to control cells within living tissue. Selected cell types are genetically modified to express light-sensitive proteins that open under light exposure and activate or inhibit the cell. This approach allows researchers to manipulate cellular events with high temporal precision.

Specifically, in the realm of neuroscience, optogenetic stimulation of neurons has revolutionized the study of brain function as it has several advantages compared to traditional methods such as direct electrical stimulation. Unlike electrical methods that lack cell-type specificity and can unintentionally activate neighboring cells or fibers of passage, optogenetics offers high spatial and temporal precision, allowing for the targeted control of specific cell types within neural circuits (Boyden et al., 2005). This precision enables researchers to investigate the contributions of specific cell types and connections to neural circuit functions. The ability to control neuronal activity with such precision and specificity has made optogenetics a powerful tool in neuroscience research, contributing significantly to our understanding of complex brain functions underlying behavior and disease, laying the groundwork for potential therapeutic strategies for neurological and psychiatric disorders (Deisseroth, 2015; Emiliani et al., 2022).

2.3.1 Channelrhodopsin

Channelrhodopsins (ChR), light-sensitive ion channels derived from green algae (genus *Chlamydomonas*), allow neurons in which they are expressed to be acti-

vated or inhibited by specific wavelengths of light. Channelrhodopsin-2 (ChR2), a faster and more sensitive variant of the original protein, has been the most widely used optogenetic actuator (Fig. 2.4-A).

After the absorption of a photon by the ChR2 all-trans-retinal (chromophore), it transforms its conformation to 13-cis-retinal, which further drives a conformational change in the channel, resulting in pore opening. ChR2 is a non-specific cation channel, letting H^+, Na^+, K^+, and Ca^{2+} ions pass through the cell's membrane, which causes rapid depolarization when expressed in a neuron's membrane. The channel is open until 13-cis-retinal relaxes back to all-trans-retinal (Bamann et al., 2008). Which specific cation transfers is determined by the electrical gradient and the channel's preference, which follows the order of cations listed (Schneider et al., 2015; Yang et al., 2019).

ChR2 gating can be described by a model with four states, **two open** and **two closed**. The model depicts the transitioning of the protein structure between those states depending on light illumination (see Fig. 2.4-B). (Nikolic et al., 2009; Foutz et al., 2012)

Various other light-sensitive proteins have been explored and developed to replicate or extend the functionality of ChR2, for example, aiming to achieve different spectral sensitivities, ion conductance properties, and kinetic behaviors, thus enhancing the methodologies available for optogenetic stimulation.

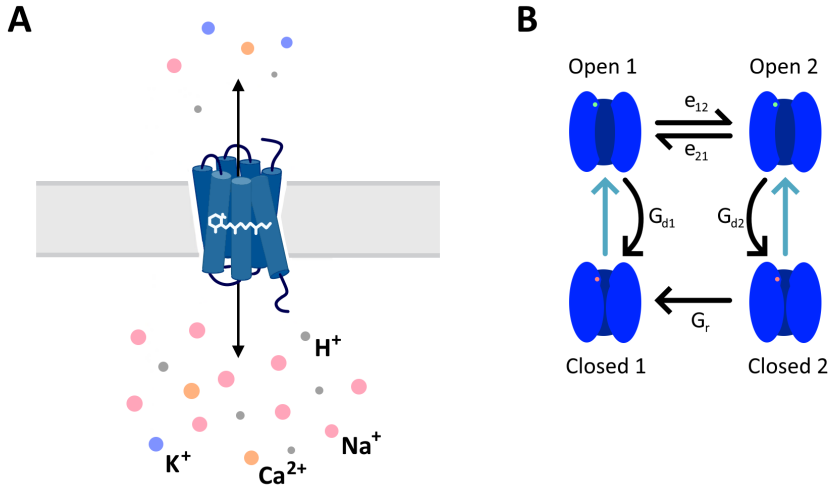

Figure 2.4: **Channelrhodopsin-2 structure and its gating characterized as a model transitioning between four states. (A)** ChR2 structure expressed in a neuron's membrane with cations flowing in both directions. A sketch of the chemical structure (in white) displays the chromophore contained within the channel. Adapted from Emiliani et al., 2022 under CC BY 4.0. **(B)** Four-state model of ChR2 gating mechanism and their transition rate constants as described by Nikolic et al., 2009 and Foutz et al., 2012. Arrows signify transitions between states - blue arrows describe channel opening in response to light exposure.

2.4 Depolarization block

Subjecting the neuron to strong sustained excitatory stimuli leads to a state in which it is unable to produce additional APs, making the neuron inactive, prohibiting signal propagation (Mattis et al., 2012; Herman et al., 2014; Tadres et al., 2022). This condition is not limited to an experimental setting - it can be achieved with a few hundred excitatory dendritic synapses (around 180) of random background activity, suggesting frequent occurrence *in vivo* (Bianchi et al., 2012). It was further tested that the activity of inhibitory synapses does not have a significant role in countering the excitatory synapses' activity, thus labeling DpB a robust phenomenon.

2.4.1 Dynamics of depolarization block

DpB can be characterized by a voltage trace with an initial burst of spiking activity, which then settles at a constantly depolarized level, the equilibrium potential, around -40 mV. To review and understand the mechanisms driving this behavior, we primarily discuss findings described in the article "*On the mechanisms underlying the depolarization block in the spiking dynamics of CA1 pyramidal neurons.*" (Bianchi et al., 2012)

How different sets of ionic currents contribute to the neuron's response to prolonged depolarization, particularly identifying the specific ion channel properties and their kinetics, was explored using morphologically realistic models of CA1 pyramidal neurons and simplified, reduced, single-compartment models. It has been shown that properties of delayed rectifier K^+ (K_{DR}) and transient Na^+ (NaT) ionic currents alone are sufficient to explain DpB dynamics.

Results have shown that these channel activation properties make neurons **more vulnerable to DpB**:

- **large window current**, a consistent current occurring in an interval of membrane voltage, where the NaT channel is neither fully activated nor inactivated, which consequently produces **considerable Na^+** current.
- **weak activation of K_{DR}**, which fails to let the neuron repolarize properly

These conditions can be equivalently viewed as happening because of how activation or inactivation of the following channels depends on voltage and time:

- **incomplete return of NaT channels to fully de-inactivated state** between APs, which results in the unavailability of a sufficient portion of NaT channels capable of firing additional AP and consequently leads to DpB
- **high voltage needed for K_{DR}** activation impedes the ability to repolarize the membrane after each AP

Both conditions together generate a progressive reduction in the NaT channel's ability to generate AP at full amplitude, subsequently triggering DpB (see Fig. 2.5). Strong K_{DR} activation is able to counteract large window current. This lets the neuron repolarize properly and avoids DpB completely (shown in Fig. 2.6)

- however, any additional depolarizing current drives DpB in this scenario. In general, these additional currents, e.g., synaptic input or different channel's current, modulate the onset of DpB but are not strictly necessary since the main effect can be explained only by **the interaction of NaT and K_{DR}**.

DpB dynamics can be influenced by other factors. Bianchi et al., 2012 have found that neurons with varying morphology differ in their electrophysiological responses and, therefore, have different threshold currents inducing DpB. Further variation of a neuron's susceptibility to DpB may be caused by different ion channel kinetics. These electrophysiological properties may further change throughout each cell's lifetime (Bear et al., 2016). Consequently, the susceptibility to DpB is distinct among individual cells, depends on the neuronal type, and may vary over the neuron's lifetime.

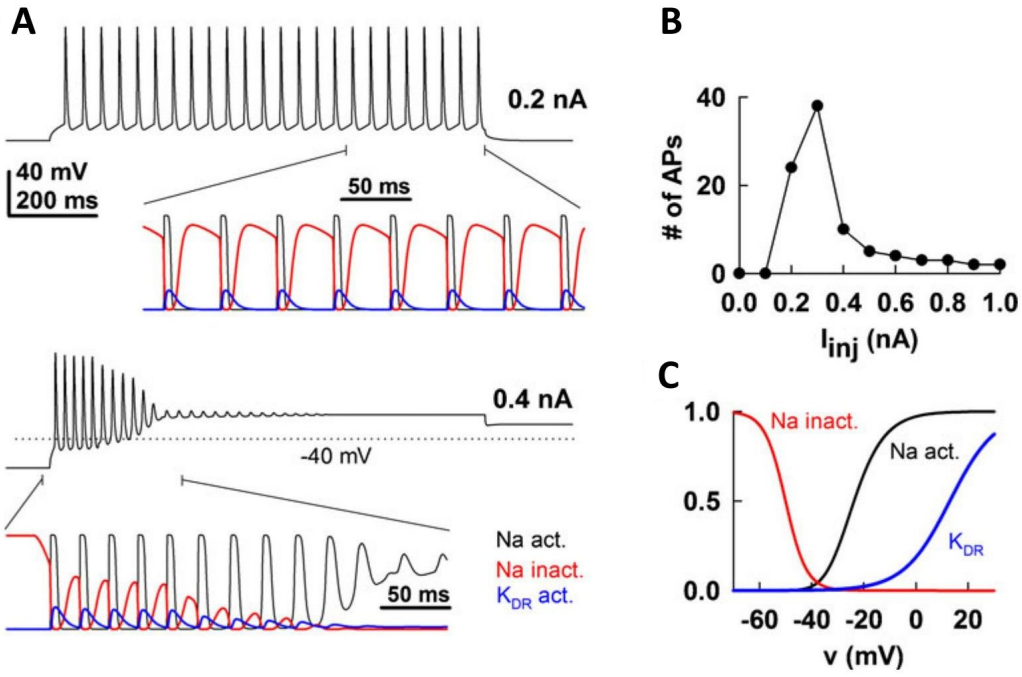

Figure 2.5: **NaT and K_{DR} currents are sufficient to drive the depolarization block. (A)** Model response to somatic current injections of 0.2 nA and 0.4 nA. Somatic membrane potential and corresponding NaT (inactivation: red, activation: black) and K_{DR} (activation: blue) gating variables during the simulation. The soma and dendrites were uniformly distributed with NaT, K_{DR} and leak currents. **(B)** Number of APs elicited in response to increasing somatic current injection. **(C)** Voltage-dependence of the steady-state activation and inactivation curves of NaT and K_{DR} sufficient to drive DpB. Figure taken from Bianchi et al., 2012 with permission of the Copyright Clearance Center.

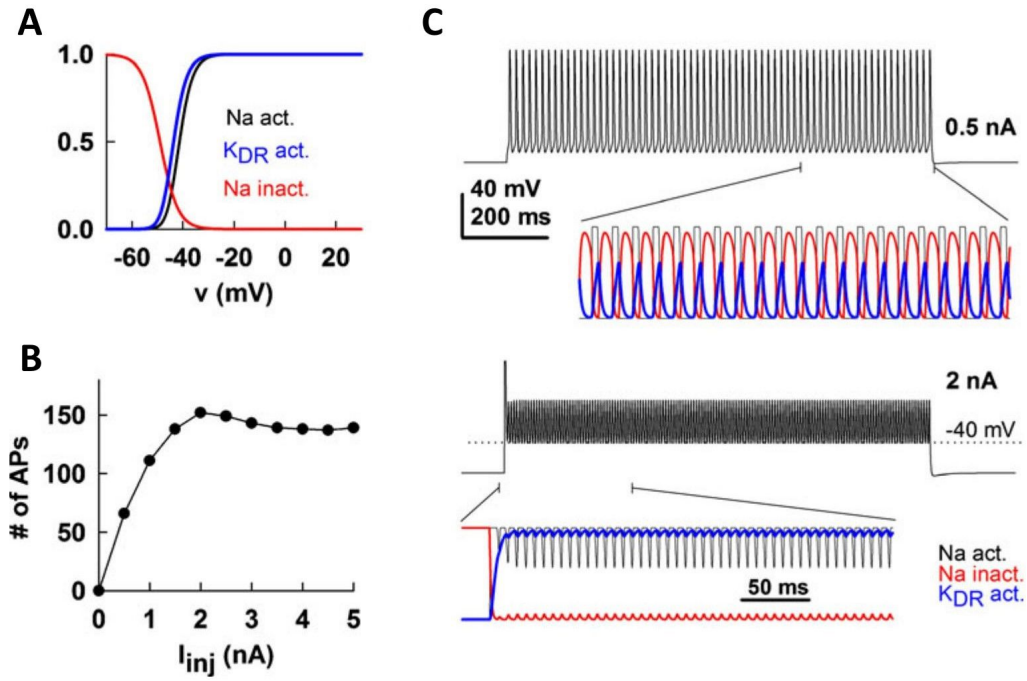

Figure 2.6: **Specific relations between NaT and K_{DR} current prevent depolarization block. (A)** Voltage-dependence of the steady-state activation and inactivation curves of NaT (inactivation: red, activation: black) and K_{DR} (activation: blue), which cannot induce DpB. **(B)** Number of APs elicited in response to increasing somatic current injection. **(C)** Model response to somatic current injections of 0.5 nA and 3 nA. Somatic membrane potential and corresponding NaT and K_{DR} gating variables during the simulation. Figure taken from Bianchi et al., 2012 with permission of the Copyright Clearance Center.

2.4.2 Kinetics across different neuronal subtypes

Apart from trying to find links between specific single-cell differences and electrophysiological behavior, there have been attempts to identify how differences in response patterns are related to neuronal subtypes. This has proven itself to be difficult since even within a subtype, there can be great biological diversity present and, therefore, varied reactions. However, even though DpB does not occur similarly across individual cells, it is possible to find parallels in how different classes of neurons respond, given shared characteristics in firing dynamics, channel composition, and membrane properties. Some of these differences make certain neuronal subtypes less resistant to DpB, see Sect. 2.4.1 for examples. (Bianchi et al., 2012; Bear et al., 2016)

This section discusses relevant findings from the article titled "*Cell type-specific and time-dependent light exposure contribute to silencing in neurons expressing Channelrhodopsin-2*". In this study, Herman et al. examine different neuronal subtypes for their susceptibility to DpB. Among them are: **interneurons** - neurons found in the central nervous system, which relay and process information (Kepecs and Fishell, 2014) - and **principal excitatory neurons**, predominant excitatory cells in the brain, serving as key integrators and transmitters of information (Bear et al., 2016). These neurons were stimulated with

20 regular light pulses, starting 50 ms after each other. The pulse-width ranged from 1 ms to 49 ms, with the latter being similar to continuous light stimulation, which is the stimulation protocol we focus on in this thesis. (Herman et al., 2014)

The study finds that **interneurons**, highly diverse, are of greater vulnerability to **light-induced DpB** than **principal excitatory neurons**, which display higher resistance to it. Further, they discover that, out of subtypes studied, interneurons exhibiting responsive high-frequency generation of APs, i.e., **fast-spiking interneurons**, are more resistant to DpB than **regular-spiking interneurons**. For the more resistant fast-spiking interneurons, their robustness to DpB can even exceed the robustness of pyramidal neurons (Mattis et al., 2012; Herman et al., 2014).

Interneurons examined were CRH, ChAT, and SST interneurons, termed by the specific proteins that these cells express (protein markers). However, even within the interneuronal subtypes listed, variability of neuronal responses was still observed (e.g., in Fig. 2.7). This stems from different gene expression patterns, which are known to be variable between brain areas as well, suggesting that categorization based on broad protein markers alone may not be generalizable from one brain region to another.

The analysis reveals that firing rates of all interneurons have increased with increasing light intensity (10 to 40 mW/mm^2), and with increasing pulse duration, they were driven into DpB regardless of intensity. However, fast-spiking SST interneurons exhibited increased and persistent firing at all pulse durations and intensities tested. With almost continuous light stimulation, there was an initial burst of APs followed by DpB in regular-spiking interneurons and higher spiking integrity in fast-spiking SST interneurons (Fig. 2.7).

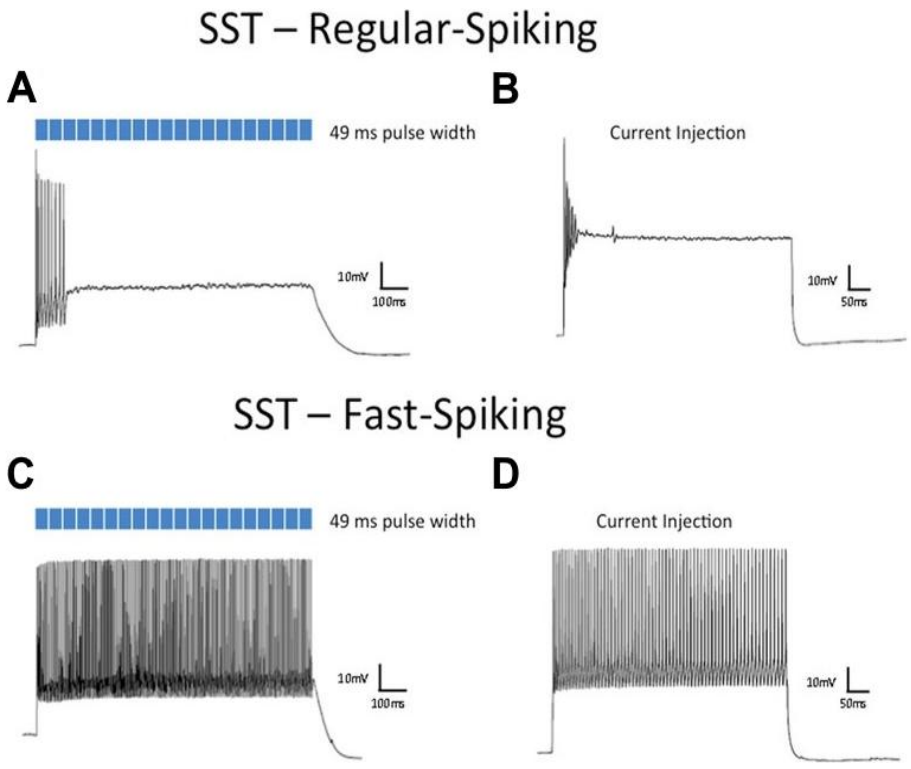

Figure 2.7: **Effects of light and current stimulations on a heterogeneous SST interneuron population.** Regular-spiking ChR2-expressing SST cortical interneuron **(A)** in response to prolonged light pulse duration (20 Hz, 49 ms pulse width) leads to DpB, analogously to **(B)** high current injection (100 pA). Fast-spiking SST cortical interneuron **(C)** in response to prolonged light pulse duration (20 Hz, 49 ms pulse width) leads to robust firing, analogously to **(D)** high current injection (500 pA). Taken and edited from Herman et al., 2014 distributed under the terms of the Creative Commons Attribution License.

Principal excitatory neurons studied were **L5 pyramidal neurons** (primary excitation units of the mammalian prefrontal cortex and corticospinal tract) and **mitral cells** (part of the olfactory system) (Dryer and Graziadei, 1994). Both types are consistently more resistant to light-induced DpB than interneurons. Excitatory neurons, mostly **larger** than interneurons, have **lower membrane resistance** as a direct consequence of their larger size. This makes them more resilient to current-induced DpB, as changes in voltage across the membrane require higher levels of input. It is, however, only hypothesized that their resilience to light-induced DpB also originates from their size.

Mitral cells were the most resistant to light-induced DpB out of the neurons studied. Interestingly, fast-spiking SST interneurons, which were the most robust among interneurons, matched in their response to mitral cells. Consequently, fast-spiking neurons and mitral cells were most robust, followed by L5 pyramidal neurons, rendering the remaining interneurons sensitive to DpB.

In summary, specific populations of seemingly homogenous neurons in the same brain region may exhibit dramatically different firing behaviors and, thus,

different susceptibilities to DpB. On the other hand, shared characteristics of neuronal dynamics within classes of neurons can be outlined as well. The study suggests that all excitatory cells are commonly less susceptible to DpB due to their size. Conversely, interneurons are, on average, more vulnerable to this phenomenon than principal excitatory cells. At almost continuous light stimulation, it has been shown that, out of the cells studied, principal excitatory cell types and fast-spiking interneurons are the most resistant to DpB.

2.4.3 Function

Its function remains not entirely understood and is subject to hypotheses. Many have labeled DpB as a pathological state or a state that is coincidental with pathological conditions, specifically seizure-like activities. (El Houssaini et al., 2015; Kim and Nykamp, 2017; Călin et al., 2021; Elsayed and El-Mallakh, 2023)

Catatonia, for example, can be conceptualized as a condition resulting from the faulty regulation of ion levels, especially due to reduced removal of Na^+ ions from the inside of cells. This increase in the intraneuronal sodium concentration elevates the membrane potential and may consequently result in sustained DpB. Researchers suggest that hyperpolarizing neurons represents the most effective treatment for catatonia. (Elsayed and El-Mallakh, 2023)

When investigating mechanisms for combating epileptic network activity, researchers tested the hypothesis that DpB in PV (parvalbumin) interneurons in the cortex is a key factor in decreasing the ability to prevent overactive neural activity during seizures. The findings revealed that epileptiform activity - abnormal activity resembling the patterns seen in epilepsy - was associated with the failure of inhibitory synaptic mechanisms and the occurrence of DpB in PV interneurons. These experiments support the notion that DpB in feedforward inhibitory synaptic mechanisms is a vulnerability point, highlighting it as a target for preventing the initiation and propagation of seizure activity. (Călin et al., 2021)

However, the therapeutic effects of DpB are known as well. Studies suggest that anti-psychotic drugs exert their influence on people with schizophrenia by causing DpB in dopaminergic neurons, thus preventing further activity and attenuating the dopamine system's responsiveness. (Grace et al., 1997; Lodge and Grace, 2011)

In contrast to the pathological role of DpB, studies have shown that DpB can enhance information encoding. The existence of two firing modes - tonic and burst (DpB) spiking - suggests more complex processing capabilities, enabling brief signals to create lasting changes in firing patterns, which may be involved in short-term memory (Dovzhenok and Kuznetsov, 2012). Further, DpB has been shown to expand the dimensionality of information encoding in olfactory sensory neurons, which enter DpB at odor concentrations significantly higher than their detection threshold. This physiological function is theorized to be common across various sensory neurons (Tadres et al., 2022).

3. Methods

This chapter provides a comprehensive overview of our methodology for assessing how changes in biophysical conditions of excitatory neurons influence neurons' susceptibility to DpB.

Since modifying the biophysical conditions of a neuron and stimulating it until it reaches DpB can be challenging in a laboratory setting, we studied this phenomenon within a computer simulation.

To create and handle computational models of neurons, we used the NEURON simulation environment (Hines and Carnevale, 2001; Carnevale and Hines, 2006) via its Python interface. To simulate optogenetic stimulation of a modeled neuron, we utilize an existing open-source software framework implementing optogenetic stimulation on top of the NEURON simulation environment (A.1.1; Aravanis et al., 2007; Nikolic et al., 2009; Foutz et al., 2012; Berling et al., 2024). For further details, we provide the code used for all the simulations within this thesis. It is accessible on GitHub (see Appendix A.1).

3.1 A simplified model for simulating neural activity

To simulate neural activity at the cellular level, we utilized an existing model of L5 pyramidal neuron, which represents one major neuron type present in the cortex. The neuron model has been developed and fine-tuned throughout various studies in the past (Mainen and Sejnowski, 1996; Hu et al., 2009) and has further been extended by a Channelrhodopsin-2 model (Foutz et al., 2012; Nikolic et al., 2009), which describes the channel's photocycles, allowing the simulation of optogenetic stimulation. All extensions together correctly model DpB (Berling et al., 2024).

Since we are interested in understanding basic mechanisms impacting the susceptibility of a neuron to DpB, we decided to tackle the complexity of the simulated L5 neuron and reduced its morphology by removing the axon and the dendritic tree, which vary among neurons (Spruston, 2008). This simplifies the model from several hundred coupled compartments to a single-compartment soma-only neuron model. Reduced complexity further reduced the computational demand of the model, enabling us to explore the parameter space more widely.

3.2 Optogenetic model setup

The setup of our optogenetic stimulation environment, simulating the soma-only neuron under light exposure, is shown in Fig. 3.1. Since we assume a uniform expression of ChR2 across the neuron's membrane *in vivo*, we distribute the channel accordingly and set the light intensity at the neuronal membrane as a parameter of our model (parameter: *irradiance / flux density*, in watt per square millimeter, W/mm^2).

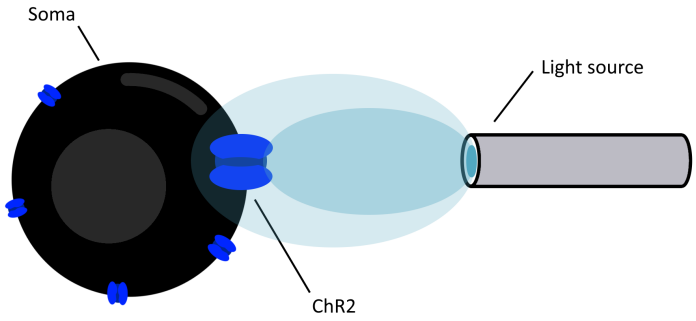

Figure 3.1: **A sketch of virtual stimulation setup of simulated soma-only neuron under light exposure.** The figure displays a soma with ChR2 channels in its membrane and a light source stimulation framework targeting it with blue-light rays.

3.3 Replicating depolarization block in the simplified model

To verify that our simplified model can simulate and correctly represent the mechanism behind DpB, as revealed by Bianchi et al., 2012, we replicated their results in our model. We, therefore, recorded the gating variables of the Na_v and K_v channels during potent optogenetic stimulation, driving the neuron into DpB, see Fig. 3.2. We found that Na_v channels do not inactivate fully, and their inactivation becomes weaker with each AP, which eventually results in the complete unavailability of Na_v channels to generate further APs (Fig. 3.2-B). As Na_v channels become unavailable for AP generation, the membrane voltage stays at a constantly depolarized value - equilibrium potential (Fig. 3.2-A). This behavior resembles the dynamics Bianchi et al., 2012 have found to underlie DpB (see Sect. 2.4.1), which demonstrates our model's capability of correctly modeling DpB.

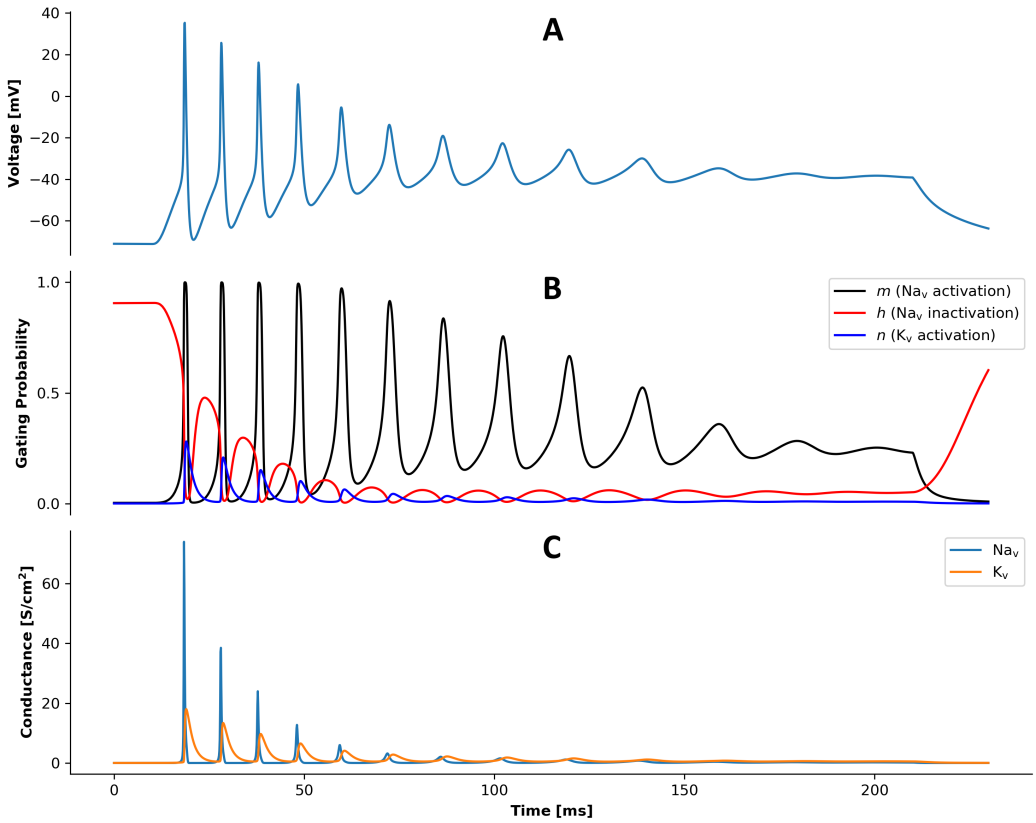

Figure 3.2: **Depolarization block response and underlying channel dynamics in the simulated simplified neuron model.** **(A)** Somatic membrane voltage trace, **(B)** channels' gating variables, and **(C)** channel-specific conductance densities during simulated optogenetic stimulation of 200 ms starting at 20 ms.

4. Results

Since Bianchi et al., 2012 demonstrated that DpB is caused by the combined dynamics of sodium and potassium ion channels (see Sect. 2.4.1), we want to explore how varying their density in the neuronal membrane affects the neuron's tendency to go into DpB.

To evaluate a neuron's susceptibility to DpB, we must measure the light intensity at which the cell goes into DpB. This requires a formal classification of the DpB condition from the simulated voltage trace. Given the classification, we perform a parameter scan across varying conductance densities of Na_v and K_v, finding that both Na_v and K_v channel conductance densities act against the neuron's susceptibility to DpB.

Hypothesizing that the size of the neuron may impact its susceptibility, we test it and find that it does not play a role.

We further observed that the equilibrium potential at which the neuron settles after the initial burst of spiking activity differs between various DpB cases. We found that this is linked to the Na_v but not the K_v channel conductance density.

4.1 Classification of depolarization block condition

Analyzing DpB occurrence in relation to the neuron's biophysical properties requires a formal definition of DpB, which has yet to be established. Scientists have so far only vaguely characterized DpB (see Sect. 2.4) - from describing it simply as "plateau potentials" (Mattis et al., 2012) to "change in the membrane potential that prevents the cell from generating action potentials" (Kameneva et al., 2016).

Bianchi et al., 2012 have suggested the most concrete definition to date. In their study, they define depolarization block to occur at any stimulation intensity exceeding the intensity at which the neuron exhibited a maximum number of APs by a certain value. The weakness of this definition is that DpB dynamics are neuron-type dependent and, therefore, adding a constant value to the stimulation intensity of the maximal response does not mark stimulation intensities, which result in comparable DpB dynamics across different neurons. Therefore, we establish our own measure to reliably compare neurons of different biophysical properties for entering the dynamically same state. We find the following criteria to reliably reduce variability within the DpB condition:

1. The first and last spike must occur before the last quarter of the stimulation period since DpB is described as a burst of APs followed by a plateau, and further,

2. the variance in the last quarter of the stimulation period must be less than 1 mV to prevent rebound of oscillations or spiking activity during the plateau, and

3. the membrane voltage mean of the last quarter of the stimulation period must be above or equal to -40 mV to prevent low threshold stimulation

intensities from being classified as inducing DpB.

Classifying DpB with only a subset of these restrictions resulted in traces lacking consistent characteristics. Using the first criterion only, yielded traces exhibiting robust spiking activity, in which AP amplitudes only narrowed towards the end of stimulation below the value that identifies an AP, and traces in which spiking activity recovered from DpB (Fig. 4.1-A). Additionally restricting the variance of membrane voltage in the last quarter of the stimulation period, successfully prevented these effects (Fig. 4.1-B). Lastly, we had to prevent that traces showing only one AP and then failing to produce another due to insufficient stimulation intensity were also classified as DpB. To combat this, we included the last criterion, which requires depolarization to be, on average, elevated to -40 mV in the last quarter of the stimulation period, in agreement with the dynamics Bianchi et al., 2012 describe.

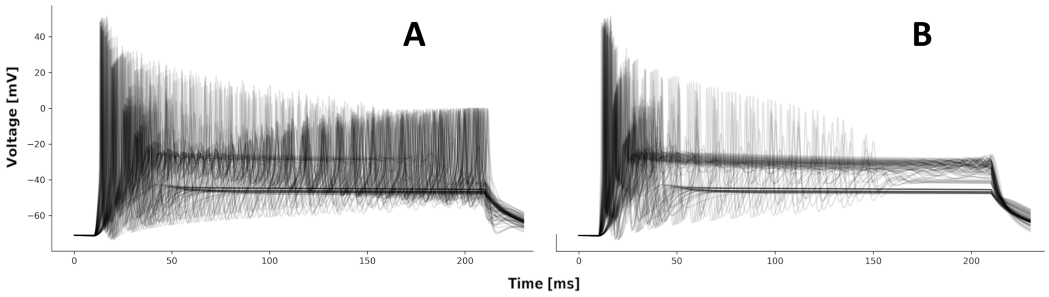

Figure 4.1: **Membrane voltage traces partially incorrectly classified as exhibiting depolarization block according to different restrictions.** Each trace of the membrane voltage over time corresponds to a neuron with modified maximum channel conductance densities under photo-stimulation. The graphs show how our classifier performs **(A)** with the first restriction only, which imposes that the first and the last spike has to occur before the last quarter of the stimulation interval, and **(B)** adds a second restriction - the membrane voltage of the last quarter of the stimulation period has to have variance less than 1 mV.

Imposing the three restrictions together successfully standardized the appearance of voltage traces for our purposes (Fig. 4.2).

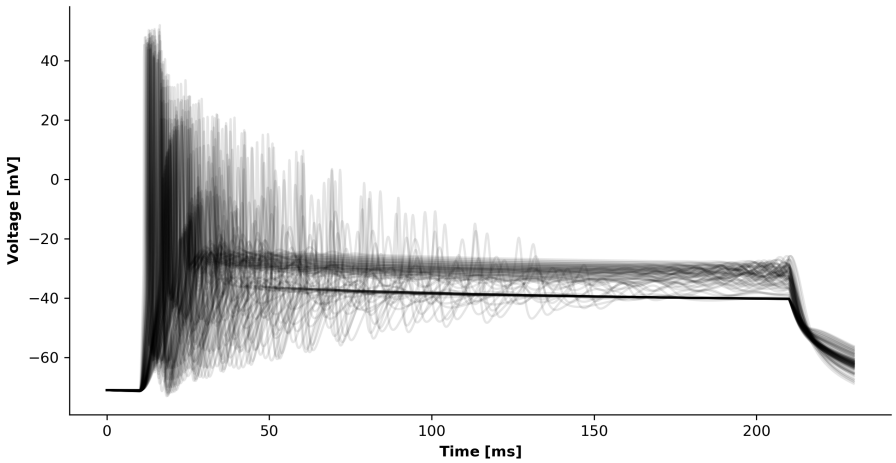

Figure 4.2: **Membrane voltage traces labeled as exhibiting depolarization block, according to a refined definition, display shared characteristics.** Each trace of the membrane voltage over time corresponds to a neuron with modified maximum channel conductance densities under potent photostimulation inducing DpB.

The final definition we arrived at can be formalized in pseudo-code:

Algorithm 1 Check if Depolarization Block Has Occurred

procedure DepolarizationBlock($voltageTrace$)
    Initialize $spikeTimes$
    Initialize $lastPortionOfStimInterval$
    if number of items in $spikeTimes$ is 0 **then**
        return $False$
    end if
    if first spike from $spikeTimes$ occurred in the first half of the stimulation **and** the last spike occurred before $lastPortionOfStimInterval$ starting time **then**
        if variance of $lastPortionOfStimInterval$ voltage < 1 **then**
            if mean of $lastPortionOfStimInterval$ voltage ≥ -40 **then**
                return True
            end if
        end if
    end if
    return $False$
end procedure

Our formalized definition, now algorithmized, enables us to determine whether the given voltage trace exhibits DpB, thus supporting the exploration of parameter space of various biophysical properties.

4.2 Stimulation intensities inducing depolarization block for varying Nav and Kv channel densities

To prevent or to purposefully induce DpB in a neuromodulation scenario, we have to fully understand trends in stimulation intensities at which DpB occurs with varying numbers of Na_v and K_v channel densities across the neuronal membrane.

For this, we modify each channel's maximum conductance density (in siemens per square centimeter, S/cm^2). Channel densities relate to conductance (denoted g) by multiplying the number of each channel by their respective conductance - therefore, the maximum conductance densities can be used interchangeably.

We established a domain space, ranging from half to twice the default values of both Na_v (default $\bar{g}_{Nav} = 256.752\ S/cm^2$) and K_v (default $\bar{g}_{Kv} = 64.188\ S/cm^2$) channel densities (default densities are uniform within the soma and are based on Hu et al., 2009). For every pair of values within this domain applied to the neuron's membrane, we identify the minimal stimulation intensity that results in a voltage trace classified as exhibiting DpB (Alg. 1). The algorithm's pseudo-code we used to search the domain space is presented as follows (Alg. 2).

Algorithm 2 Find DpB Intensities Across the Domain

```
procedure FindDpbIntensities(defaultNa_vDensity, defaultK_vDensity)
    Initialize rows ← [ ]
    Initialize domain ← all combinations of Na_v and K_v density values
    for each Na_v, K_v pair in domain do
        dpbIntensity ← BinSearchForIntensity(Na_v, K_v)
        rows.add(Na_v, K_v, dpbIntensity)
    end for
    return rows
end procedure
```

We used a modified binary search algorithm to efficiently find the correct intensity value (shown in Alg. 3). The intensity space is not discrete, so precision had to be introduced.

Algorithm 3 Find Depolarization Block Intensity

```
1: procedure BinSearchForIntensity(Na_vDensity, K_vDensity)
2:     Initialize left boundary l ← 0
3:     Initialize right boundary r ← 25000
4:     Initialize precision
5:     dpbIntensity ← r
6:     while (r − l) > precision do
7:         intensity ← the midpoint of l and r
8:         voltageTrace ← Simulate(Na_vDensity, K_vDensity, intensity)
9:         if DepolarizationBlock(voltageTrace) then
10:            dpbIntensity ← intensity
11:            r ← intensity
12:        else
13:            l ← intensity
14:        end if
15:    end while
16:    return dpbIntensity
17: end procedure
```

Our results show a clear trend that the higher the density of Na_v channels is, the harder it is to achieve the DpB. Increasing K_v channel density increases the stimulation intensity needed to induce DpB as well (Fig. 4.3).

Elevated Na_v channel density may increase the threshold of intensities at which the neuron is driven into DpB, as the increased availability of channels capable of driving membrane depolarization enhances the likelihood of generating additional APs. Higher density of K_v channels supports the flow of repolarizing current, which causes the neuron's membrane to repolarize more efficiently, thus preventing DpB. This aligns with what Bianchi et al., 2012 find (Sect. 2.4.1).

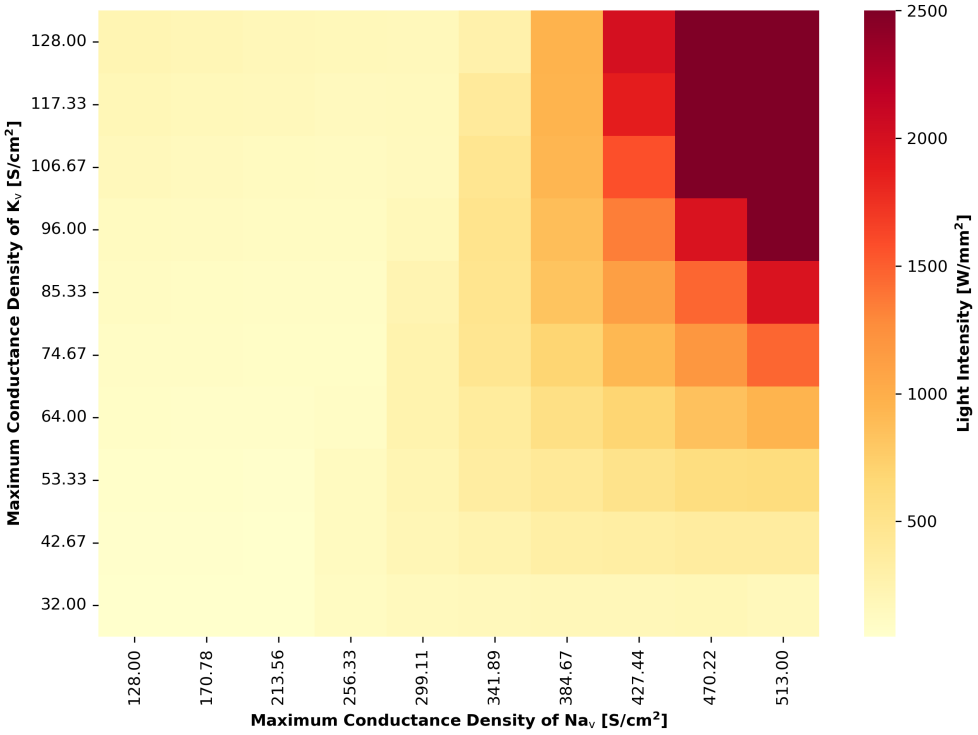

Figure 4.3: **Minimal stimulation intensities required to reach the depolarization block with given Na_v and K_v maximum conductance densities.** Conductance densities are displayed on the axes, and light intensity (irradiance) to induce DpB is color-coded. Upper-right tile values are scaled down for displaying purposes - actual values exceed the range of visualized colors.

4.3 Impact of size on neuronal response

Drawing from their findings, Herman et al., 2014 suggest that the observed greater susceptibility to light-induced DpB of interneurons in comparison to principal excitatory neurons may be explained by their smaller size.

We, therefore, further inspect stimulation intensities driving DpB in relation to the size of the simulated neuron by scaling the length of its segments without altering the Na_v and K_v channel densities.

We observed no significant effect of neuron size on susceptibility to light-induced DpB (Fig. 4.4). This finding allows us to conclude that, according to our model of optogenetic stimulation, size is not a factor influencing the electrophysiological behavior of the stimulated cells under light exposure of potent intensity. This finding contrasts with Herman et al., 2014, who argue that neuronal size directly affects susceptibility to DpB. It is known that larger neuronal size results in lower membrane resistance, demanding higher levels of **current** input to achieve sufficient depolarization. However, we have found this to be untrue within our optogenetic stimulation model, suggesting that the effects observed may depend on the stimulation technique used.

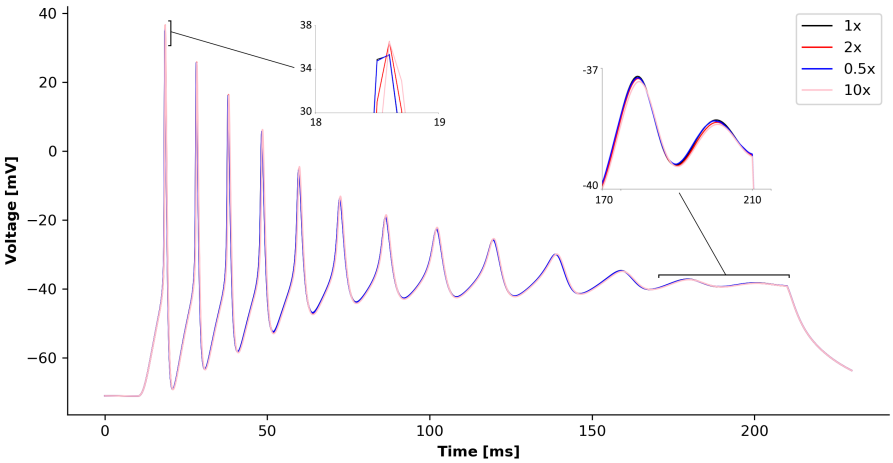

Figure 4.4: **Neurons of different sizes exhibit the same response dynamics.** *1x* shows a somatic membrane voltage trace of a neuron with default size, *2x* with size doubled, *0.5x* with half the default size, and *10x* ten times its default size. Membrane's channel densities were set to their default values.

4.4 Variance of equilibrium potential and its link to Nav and Kv channel densities

The voltage traces exhibiting DpB converge towards two specific values at the end of the stimulation period, specifically around −40 mV and −30 mV, which is in the range that Bianchi et al., 2012 find (see Fig. 4.2). We aimed to uncover if and how channel densities of Na_v and K_v channels are linked to the particular strength of equilibrium potential and whether and how these densities affect the separation of voltage traces into two distinct equilibrium potential values.

We compare the equilibrium potentials (mean values of the membrane voltage during the last quarter of the stimulation interval) relative to Na_v and K_v channel densities. We find that with higher Na_v channel density, the equilibrium potential rises (Fig. 4.5-A), while higher K_v channel density does not affect, or may slightly decrease, the mean towards the end of stimulation (Fig. 4.5-B).

At lower Na_v channel densities, the equilibrium voltage is strictly around −40 mV without any variation. However, intermediate Na_v channel densities introduce a region where K_v channel density impacts the equilibrium potential, creating wider deviation across this interval. At higher channel densities, the equilibrium potential decreases in deviation again and seems to settle around −30 mV. This suggests that both lower and higher values of Na_v channel density determine the strength of the equilibrium potential. While the equilibrium potential increases with rising intermediate values of Na_v channel densities, it also presents a region of high variance where the density of K_v channel shifts the potential value (Fig. 4.5-A).

More depolarized equilibrium potential resulting from higher Na_v channel densities can be explained by the relation of voltage-dependent steady-state activation curves of both channels (see 2.5). To induce DpB, a stronger depolarizing current, created by increasing Na_v channel density, needs to be counteracted by

an appropriately strong K_v activation. More robust activation of K_v channels occurs at higher voltage values, leading to DpB at elevated membrane potentials. Further research has to understand why there is a region of intermediate Na_v channel densities where K_v channel density impacts the equilibrium potential more substantially.

We can conclude that Na_v channel density across the simulated neuronal membrane is the driving factor influencing the equilibrium potential. However, at intermediate Na_v channel densities, K_v influences the equilibrium potential value as well.

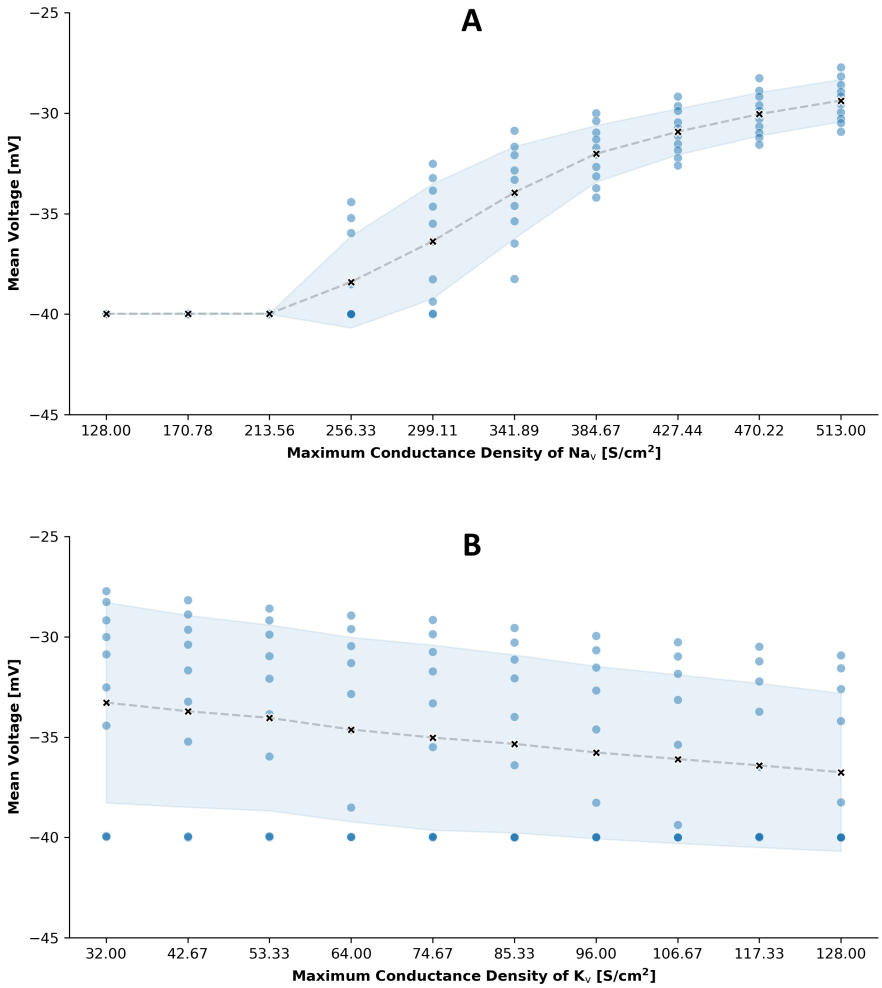

Figure 4.5: **Height of equilibrium potential towards the end of stimulation for varying Na_v and K_v channel densities.** Mean of simulated somatic membrane voltage traces in the last quarter of the stimulation period (y-axis) is shown in relation to specific channel densities (x-axis). Each dot corresponds to an equilibrium potential of a neuron with unique Na_v and K_v channel density. The silver dashed line shows connected averages, and the light blue band shows a standard deviation from it. Graph **(A)** displays mean equilibrium membrane voltage plotted against Na_v channel density and **(B)** against K_v channel density.

5. Conclusion

In this thesis, we studied how the biophysical properties of excitatory neurons affect the cell's susceptibility to enter depolarization block (DpB). While DpB can be triggered through synaptic input physiologically (Bianchi et al., 2012), it can also be induced with external stimulation (Herman et al., 2014). Here, we concentrate on DpB induced by optogenetic stimulation. This technique uses light to control cells within living tissue and is widely used in neuromodulatory experiments. When applied without precaution, targeted cells can be driven into DpB. Understanding conditions that trigger DpB precisely is, therefore, essential to avoid unintended outcomes.

We review the structure and function of an excitatory neuron and its ability to generate action potentials (APs), highlighting the role of voltage-gated sodium (Na_v) and potassium channels (K_v). To enable a computational approach to study DpB, we delineate a mathematical model used to describe membrane dynamics of excitable cells - the Hodgkin-Huxley conductance-based model, which captures how APs are initiated and propagated (Hodgkin and Huxley, 1952). Further, we utilize a model of the light-sensitive protein Channelrhodopsin-2 (ChR2) (Nikolic et al., 2009), which, in combination with the Hodgkin-Huxley neuron model, allows us to simulate the optogenetic stimulation of a neuron.

We further review the biological background and the mechanisms behind DpB dynamics as mathematically described by Bianchi et al., 2012, who show that specific Na_v and K_v channel-dynamics are sufficient for DpB to arise. However, DpB dynamics are not uniform across neurons - Herman et al., 2014 demonstrate that different neuronal subtypes exhibit diverse responses when subjected to potent stimulation. The study finds that interneurons are, on average, more susceptible to DpB than principal excitatory cells and hypothesizes that this higher susceptibility may be linked to the interneuron's smaller size.

To simulate DpB induced through optogenetic stimulation, we simplify an existing neuron model of a layer V (L5) pyramidal neuron, for which an optogenetic stimulation model already exists (Berling et al., 2024). Our simplification reduces the original model with complex morphology represented by many compartments to a single-compartment model, resulting in a generic model of an excitatory neuron's soma. We then verify that its DpB dynamics match the findings reported by Bianchi et al., 2012. Using the model and established background, we address the following issues:

- **G_0:** To understand how certain biophysical properties affect the neuron's susceptibility to DpB and compare them across a wide parameter space, we required a robust classification of DpB from a simulated voltage trace. However, current research defines DpB only vaguely. We, therefore, came up with a formalized definition and automatic voltage-trace classification ourselves, allowing for a systematic comparison of conditions triggering consistently similar DpB dynamics. (Sect. 4.1)

- **G_1:** Linking neuronal properties like membrane channel densities with a cell's electrophysiological responses allows us to conduct experiments in a more informed manner. We investigate channels that are known to explain

DpB dynamics and find that increasing Na_v or K_v channel densities makes the neuronal membrane more refractory to light-induced DpB. This can be mechanistically understood as follows: Increasing Na_v channel density provides the neuron with more depolarizing current available in the relative refractory period, thus aiding in the generation of another AP. Higher K_v channel densities aid in repolarizing the membrane after rapid depolarization, returning to a state from which another AP can arise. (Sect. 4.2)

- **G_2:** To test if the size of the simulated neuron plays a role in its resistance to DpB, as Herman et al., 2014 have suggested, we simulate optogenetic stimulation of the same neuron with varied size. We find that it has no effect on light-induced DpB. This suggests that the size of neurons is not the factor making interneurons less resistant to light-induced DpB than excitatory ones, as the study suggested. (Sect. 4.3)

- **G_3:** Voltage traces classified as DpB, according to our classification introduced in G_0, exhibited similar dynamics except for different equilibrium potentials. We test whether and how Na_v and K_v channel densities affect the membrane voltage value at which the trace plateaus, finding that increasing Na_v channel density increases the equilibrium potential, while increasing K_v channel density has almost no effect. Higher equilibrium potential for increasing Na_v channel density can be explained by the more robust K_v channel activation required to counteract stronger depolarizing current and induce DpB. Since stronger voltage-dependent activation of K_v channels is achieved at higher membrane voltage values, so is the equilibrium potential. While both lower and higher densities of Na_v channels determine the value of equilibrium potential without the influence of K_v channel density, for intermediate values of Na_v channel densities K_v channel density displays a more significant impact on where the membrane voltage trace plateaus. (Sect. 4.4)

5.1 Discussion

To enable efficient computational analysis, we had to introduce a formal definition of the DpB condition. The set of restrictions upon the simulated membrane voltage traces, which for our purposes classifies whether the block occurred, is not universal, and a slight change in it could potentially lead to different results, directly depending on the established definition. However, the arbitrary selection of membrane voltage thresholds and amplitude variance restrictions during DpB classification results only in quantitative and no qualitative differences to the results we obtained.

Even after reduction, enabling us to explore our parameter space efficiently, and verified fundamental dynamics, there are further limitations to our computational model. While common, the use of ChR2 in our experiments limits the generalizability of our findings and may not directly translate to other channels used for optogenetic stimulation. Exploring other opsins with varying kinetics and gating mechanisms might alter the cellular response (Mattis et al., 2012). Our analysis, therefore, demands to be expanded and tested with different opsins.

Secondly, our model relies on continuous light stimulation. Even though this provides a solid foundation for our exploratory analysis, including pulse-width and pulse-frequency as other dimensions to the parameter space is, therefore, a logical next step. Additionally, it was found that employing shorter pulse widths helps to minimize unintentional neuronal silencing (Herman et al., 2014), possibly giving the neuron time to repolarize properly. Future work should treat the problem with pulsed stimulation.

Thirdly, different neuronal responses might arise when photo-stimulating various parts of the neuron's morphology. Stimulating neurons without their complex morphology taken into account potentially oversimplifies their actual electrophysiological behavior. Future studies should consider the intricate structures of neuronal dendrites and arbors to capture neuronal responses in their full complexity.

While DpB is considered to play a role in various disease-like states, for example, disrupting the usual activity of inhibitory neurons, potentially leading to destabilization of the whole system and subsequent epileptic activity (Călin et al., 2021), it also exerts significant influence on information encoding, expanding sensory neurons' processing capabilities (Tadres et al., 2022), and neural circuit dynamics (Dovzhenok and Kuznetsov, 2012; Kim and Nykamp, 2017). With our single-cell model, the impact of our work is limited to refining stimulation techniques. In the future, network modeling would be worth exploring to investigate the impact of DpB on broader neural functions.

Identifying specific characteristics of cells that influence their membrane responses in a predictable way is crucial for understanding how to approach specific neuronal subtypes in experiments. Findings from Herman et al., 2014 suggest that fast-spiking neurons are innately more resistant to DpB than regular-spiking neurons. We hypothesize that neurons with voltage-dependent activation curves of Na_v and K_v close to each other exhibit high-frequency firing rates (fast-spikingness). Their resistance to DpB can be explained by strong K_v activation counteracting rapid Na_v activation. This repolarizes the neuron properly for another AP to arise, thus preventing DpB. Further investigation is required to confirm this.

Our simulations of different neuron sizes demonstrated that neuronal size does not influence response consistency and, therefore, did not alter susceptibility to light-induced DpB. This is contrary to what Herman et al., 2014 conclude from their recordings across various neuron types under optogenetic stimulation, in which larger neurons were more resistant to DpB than smaller ones. Even though they argue that lowered membrane resistance makes larger neurons less vulnerable, we find this to be untrue in our computational model. While increased membrane area indeed lowers the membrane resistance, which in turn requires higher stimulating currents to drive depolarization, a larger membrane area also results in a higher number of ChR2 expressed in the neuronal membrane, which results in higher stimulating current compensating the lowered membrane resistance. We, therefore, conclude that given similar densities of ChR2 in the membranes of different neuronal subtypes, neuron size does not impact the resistance to DpB, and there was a confounding variable underlying the observations of Herman et al., 2014.

5.2 Impact

This thesis explores the impact of the biophysical properties of excitatory neurons on their susceptibility to DpB when exposed to optogenetic stimulation. It delves into how Na_v and K_v channels, which are the key mechanisms governing DpB dynamics, influence the neuron's ability to resist DpB. We use a computational model of a L5 pyramidal neuron, which we simplified to a single-compartment model to represent the generalized behavior of a generic excitatory neuron. The research introduces a formal definition of DpB to consistently identify DpB through voltage trace analysis, allowing for a parameter scan of various Na_v or K_v channel densities in the neuron's membrane. We discover that increasing Na_v or K_v channel densities enhances the neuron's membrane resistance to DpB. Contrary to prior studies, neuron size was found not to affect susceptibility to light-induced DpB. Furthermore, our analysis shows that both lower and higher densities of Na_v channel determine the equilibrium potential value without any significant influence of K_v channel density. However, equilibrium potentials of neuronal membranes with intermediate densities of the Na_v channel are impacted by the densities of the K_v channel more significantly. Taken together, while increasing Na_v channel density raises the voltage where DpB plateaus, K_v channel density has minimal influence on this property, except when the membrane contains intermediate densities of Na_v channels.

The insights gained from exploring and understanding the biophysical properties that trigger DpB have substantial implications. They enable researchers to design experiments more effectively, thus preventing accidental neuronal silencing, or, on the other hand, they allow targeted neuronal suppression. DpB is not restricted to an experimental setting and is likely involved in many physiological mechanisms, such as information encoding or epilepsy and other disease-related processes. Understanding DpB and conditions influencing it in neuromodulation scenarios could advance the development of visual prosthetics and generally address challenges in neural engineering, marking important progress in both medical practice and research.

References

Bruce Alberts. *Molecular biology of the cell*. W.W. Norton & Company, seventh edition, international student edition edition, 2022. ISBN 9780393884821.

Alexander M Aravanis, Li-Ping Wang, Feng Zhang, Leslie A Meltzer, Murtaza Z Mogri, M Bret Schneider, and Karl Deisseroth. An optical neural interface:in vivocontrol of rodent motor cortex with integrated fiberoptic and optogenetic technology. *Journal of Neural Engineering*, 4, 2007. ISSN 1741-2552. doi: 10.1088/1741-2560/4/3/s02.

Christian Bamann, Taryn Kirsch, Georg Nagel, and Ernst Bamberg. Spectral characteristics of the photocycle of channelrhodopsin-2 and its implication for channel function. *Journal of Molecular Biology*, 375, 2008. ISSN 0022-2836. doi: 10.1016/j.jmb.2007.10.072.

John Martin Barrett, Rolando Berlinguer-Palmini, and Patrick Degenaar. Optogenetic approaches to retinal prosthesis. *Visual Neuroscience*, 31, 2014. ISSN 1469-8714. doi: 10.1017/s0952523814000212.

Mark F. Bear, Barry W. Connors, and Michael A. Paradiso. *Neuroscience*. Wolters Kluwer, 4. ed. edition, 2016. ISBN 1451109547.

Alim Louis Benabid. Deep brain stimulation for parkinson's disease. *Current Opinion in Neurobiology*, 13, 2003. ISSN 0959-4388. doi: 10.1016/j.conb.2003.11.001.

David Berling, Luca Baroni, Antoine Chaffiol, Gregory Gauvain, Serge Picaud, and Ján Antolík. Consequences of neuronal morphology for spatially precise optogenetic stimulation. 2024. doi: 10.1101/2024.03.18.585466.

Daniela Bianchi, Addolorata Marasco, Alessandro Limongiello, Cristina Marchetti, Helene Marie, Brunello Tirozzi, and Michele Migliore. On the mechanisms underlying the depolarization block in the spiking dynamics of CA1 pyramidal neurons. *Journal of Computational Neuroscience*, 33, 2012. ISSN 1573-6873. doi: 10.1007/s10827-012-0383-y.

Edward S Boyden, Feng Zhang, Ernst Bamberg, Georg Nagel, and Karl Deisseroth. Millisecond-timescale, genetically targeted optical control of neural activity. *Nature Neuroscience*, 8, 2005. ISSN 1546-1726. doi: 10.1038/nn1525.

Nicholas T. Carnevale and Michael L. Hines. *The NEURON Book*. Cambridge University Press, 2006. ISBN 9780511541612. doi: 10.1017/cbo9780511541612.

Alexandru Călin, Andrei S. Ilie, and Colin J. Akerman. Disrupting epileptiform activity by preventing parvalbumin interneuron depolarization block. *The Journal of Neuroscience*, 41, 2021. ISSN 1529-2401. doi: 10.1523/jneurosci.1002-20.2021.

Karl Deisseroth. Optogenetics: 10 years of microbial opsins in neuroscience. *Nature Neuroscience*, 18, 2015. ISSN 1546-1726. doi: 10.1038/nn.4091.

Andrey Dovzhenok and Alexey S. Kuznetsov. Exploring neuronal bistability at the depolarization block. *PLoS ONE*, 7, 2012. ISSN 1932-6203. doi: 10.1371/journal.pone.0042811.

L. Dryer and P.P.C. Graziadei. Mitral cell dendrites: a comparative approach. *Anatomy and Embryology*, 189, 1994. ISSN 1432-0568. doi: 10.1007/bf00185769.

Kenza El Houssaini, Anton I. Ivanov, Christophe Bernard, and Viktor K. Jirsa. Seizures, refractory status epilepticus, and depolarization block as endogenous brain activities. *Physical Review E*, 91, 2015. ISSN 1550-2376. doi: 10.1103/physreve.91.010701.

Omar H. Elsayed and Rif S. El-Mallakh. Catatonia secondary to depolarization block. *Asian Journal of Psychiatry*, 84, 2023. ISSN 1876-2018. doi: 10.1016/j.ajp.2023.103543.

Valentina Emiliani, Emilia Entcheva, Rainer Hedrich, Peter Hegemann, Kai R. Konrad, Christian Lüscher, Mathias Mahn, Zhuo-Hua Pan, Ruth R. Sims, Johannes Vierock, and Ofer Yizhar. Optogenetics for light control of biological systems. *Nature Reviews Methods Primers*, 2, 2022. ISSN 2662-8449. doi: 10.1038/s43586-022-00136-4.

Michael Forrest. Can the thermodynamic hodgkin-huxley model of voltage-dependent conductance extrapolate for temperature? *Computation*, 2, 2014. ISSN 2079-3197. doi: 10.3390/computation2020047.

Thomas J. Foutz, Richard L. Arlow, and Cameron C. McIntyre. Theoretical principles underlying optical stimulation of a Channelrhodopsin-2 positive pyramidal neuron. *Journal of Neurophysiology*, 107, 2012. ISSN 1522-1598. doi: 10.1152/jn.00501.2011.

Wulfram Gerstner, editor. *Neuronal dynamics*. Cambridge Univ. Press, 2014. ISBN 9781107060838.

Alan L Goldin. Mechanisms of sodium channel inactivation. *Current Opinion in Neurobiology*, 13, 2003. ISSN 0959-4388. doi: 10.1016/s0959-4388(03)00065-5.

Anthony A. Grace, Benjamin S. Bunney, Holly Moore, and Christopher L. Todd. Dopamine-cell depolarization block as a model for the therapeutic actions of antipsychotic drugs. *Trends in Neurosciences*, 20, 1997. ISSN 0166-2236. doi: 10.1016/s0166-2236(96)10064-3.

Alexander M. Herman, Longwen Huang, Dona K. Murphey, Isabella Garcia, and Benjamin R. Arenkiel. Cell type-specific and time-dependent light exposure contribute to silencing in neurons expressing Channelrhodopsin-2. *eLife*, 3, 2014. ISSN 2050-084X. doi: 10.7554/elife.01481.

M. L. Hines and N. T. Carnevale. Neuron: A tool for neuroscientists. *The Neuroscientist*, 7, 2001. ISSN 1089-4098. doi: 10.1177/107385840100700207.

A. L. Hodgkin and A. F. Huxley. A quantitative description of membrane current and its application to conduction and excitation in nerve. *The Journal of Physiology*, 117, 1952. ISSN 1469-7793. doi: 10.1113/jphysiol.1952.sp004764.

Wenqin Hu, Cuiping Tian, Tun Li, Mingpo Yang, Han Hou, and Yousheng Shu. Distinct contributions of nav1.6 and nav1.2 in action potential initiation and backpropagation. *Nature Neuroscience*, 12, 2009. ISSN 1546-1726. doi: 10.1038/nn.2359.

T Kameneva, M I Maturana, A E Hadjinicolaou, S L Cloherty, M R Ibbotson, D B Grayden, A N Burkitt, and H Meffin. Retinal ganglion cells: mechanisms underlying depolarization block and differential responses to high frequency electrical stimulation of on and off cells. *Journal of Neural Engineering*, 13, 2016. ISSN 1741-2552. doi: 10.1088/1741-2560/13/1/016017.

Adam Kepecs and Gordon Fishell. Interneuron cell types are fit to function. *Nature*, 505, 2014. ISSN 1476-4687. doi: 10.1038/nature12983.

Christopher M. Kim and Duane Q. Nykamp. The influence of depolarization block on seizure-like activity in networks of excitatory and inhibitory neurons. *Journal of Computational Neuroscience*, 43, 2017. ISSN 1573-6873. doi: 10.1007/s10827-017-0647-7.

Dorothy M. Kim and Crina M. Nimigean. Voltage-gated potassium channels: A structural examination of selectivity and gating. *Cold Spring Harbor Perspectives in Biology*, 8, 2016. ISSN 1943-0264. doi: 10.1101/cshperspect.a029231.

Sonja Kleinlogel, Christian Vogl, Marcus Jeschke, Jakob Neef, and Tobias Moser. Emerging approaches for restoration of hearing and vision. *Physiological Reviews*, 2020. ISSN 1522-1210. doi: 10.1152/physrev.00035.2019.

Daniel J. Lodge and Anthony A. Grace. Hippocampal dysregulation of dopamine system function and the pathophysiology of schizophrenia. *Trends in Pharmacological Sciences*, 32, 2011. ISSN 0165-6147. doi: 10.1016/j.tips.2011.05.001.

Zachary F. Mainen and Terrence J. Sejnowski. Influence of dendritic structure on firing pattern in model neocortical neurons. *Nature*, 382, 1996. ISSN 1476-4687. doi: 10.1038/382363a0.

Joanna Mattis, Kay M. Tye, Emily A. Ferenczi, Charu Ramakrishnan, Daniel J. O'Shea, Rohit Prakash, Rohit Prakash, Lisa A. Gunaydin, Minsuk Hyun, Lief E. Fenno, Viviana Gradinaru, Viviana Gradinaru, Ofer Yizhar, and Karl Deisseroth. Principles for applying optogenetic tools derived from direct comparative analysis of microbial opsins. *Nature Methods*, 2012. doi: 10.1038/nmeth.1808. URL `https://pubmed.ncbi.nlm.nih.gov/22179551`.

Christopher Miller. An overview of the potassium channel family. *Genome Biology*, 1, 2000. ISSN 1474-760X. doi: 10.1186/gb-2000-1-4-reviews0004.

Anirban Nandi, Thomas Chartrand, Werner Van Geit, Anatoly Buchin, Zizhen Yao, Soo Yeun Lee, Yina Wei, Brian Kalmbach, Brian Lee, Ed Lein, Jim

Berg, Uygar Sümbül, Christof Koch, Bosiljka Tasic, and Costas A. Anastassiou. Single-neuron models linking electrophysiology, morphology, and transcriptomics across cortical cell types. *Cell Reports*, 40, 2022. ISSN 2211-1247. doi: 10.1016/j.celrep.2022.111176.

Konstantin Nikolic, Nir Grossman, Matthew S. Grubb, Juan Burrone, Chris Toumazou, and Patrick Degenaar. Photocycles of Channelrhodopsin-2. *Photochemistry and Photobiology*, 85, 2009. ISSN 1751-1097. doi: 10.1111/j.1751-1097.2008.00460.x.

José-Alain Sahel, Elise Boulanger-Scemama, Chloé Pagot, Angelo Arleo, Francesco Galluppi, Joseph N. Martel, Simona Degli Esposti, Alexandre Delaux, Jean-Baptiste de Saint Aubert, Caroline de Montleau, Emmanuel Gutman, Isabelle Audo, Jens Duebel, Serge Picaud, Deniz Dalkara, Laure Blouin, Magali Taiel, and Botond Roska. Partial recovery of visual function in a blind patient after optogenetic therapy. *Nature Medicine*, 27, 2021. ISSN 1546-170X. doi: 10.1038/s41591-021-01351-4.

Franziska Schneider, Christiane Grimm, and Peter Hegemann. Biophysics of channelrhodopsin. *Annual Review of Biophysics*, 44, 2015. ISSN 1936-1238. doi: 10.1146/annurev-biophys-060414-034014.

Julian Seifter, Austin Ratner, and David Sloane. *Concepts in medical physiology*. Lippincott Williams & Wilkins, 2005. ISBN 078174489X.

Nelson Spruston. Pyramidal neurons: dendritic structure and synaptic integration. *Nature Reviews Neuroscience*, 9, 2008. ISSN 1471-0048. doi: 10.1038/nrn2286.

David Tadres, Philip H. Wong, Thuc To, Jeff Moehlis, and Matthieu Louis. Depolarization block in olfactory sensory neurons expands the dimensionality of odor encoding. *Science Advances*, 8, 2022. ISSN 2375-2548. doi: 10.1126/sciadv.ade7209.

Ting Yang, Wenying Zhang, Jie Cheng, Yanhong Nie, Qi Xin, Shuai Yuan, and Yusheng Dou. Formation mechanism of ion channel in channelrhodopsin-2: Molecular dynamics simulation and steering molecular dynamics simulations. *International Journal of Molecular Sciences*, 20, 2019. ISSN 1422-0067. doi: 10.3390/ijms20153780.

Frank H. Yu and William A. Catterall. Overview of the voltage-gated sodium channel family. *Genome biology*, 4, 2003. ISSN 1474-7596. doi: 10.1186/gb-2003-4-3-207. URL `https://europepmc.org/articles/PMC153452?pdf=render`.

List of Abbreviations

AP	Action Potential
ChAT	Choline Acetyltransferase
ChR2	Channelrhodopsin-2
CRH	Corticotropin-Releasing Hormone
DpB	Depolarization Block
K_{DR}	K^+ channel with Delayed Rectifier conductance
K_v	Voltage-gated K^+ channel
L5	Layer V
NaT	Na^+ channel with Transient current
Na_v	Voltage-gated Na^+ channel
SST	Somatostatin

A. Attachments

A.1 Code

A.1.1 Environment

Repository implementing optogenetic stimulation on top of the NEURON simulation environment:
`https://github.com/dberling/simneurostim`

A.1.2 Analysis

Scripts used for analysis are accessible on GitHub at:
`https://github.com/tobiasmarek/simneurostim-analysis`